water

MDPI

Article

Flood Vulnerability Assessment of an Urban Area: A Case Study in Seoul, South Korea

Seonmi Lee [1], Youngje Choi [2], Jungwon Ji [1], Eunkyung Lee [1], Sooyeon Yi [3] and Jaeeung Yi [1,*]

[1] Department of Civil Systems Engineering, Ajou University, 206 Worldcup-ro, Yeongtong-gu, Suwon 16499, Republic of Korea; sunki7070@ajou.ac.kr (S.L.); log58@ajou.ac.kr (J.J.); oplk100@ajou.ac.kr (E.L.)
[2] Department of Hydro Science and Engineering Research, Korea Institute of Civil Engineering and Building Technology, 283 Goyang-daero, Ilsanseo-gu, Goyang 10223, Republic of Korea; dhfodhs@kict.re.kr
[3] Landscape Architecture & Environmental Planning, University of California, Berkeley, CA 94720, USA; sooyeon@berkeley.edu
* Correspondence: jeyi@ajou.ac.kr; Tel.: +82-31-219-2507

Abstract: Climate change has led to frequent and extreme flooding events in urban areas such as Seoul, a city that is particularly vulnerable due to drainage systems that were not originally designed to handle such conditions. This study aims to develop region-specific storm risk matrices for the 25 districts in Seoul and predict storm risks. By accounting for local meteorological and geographic characteristics, these matrices will enable a more targeted approach to issuing heavy rainfall warnings, as opposed to the current nationwide system. The methodology involves calculating entropy weight based on various factors, assessing flood vulnerability, and estimating region-specific rainfall associated with warning levels. These warning levels are then used to create storm risk matrices, which are tested for conformity against historical flood events. Finally, a storm risk prediction technique is developed using rainfall forecasting data. Results demonstrate the feasibility of using the newly developed storm risk matrices to predict flood damage up to 72 h in advance. This greatly contributes to the development of effective mitigation plans for addressing climate change-driven urban flood damage. The study's findings offer valuable insights for enhancing local-specific heavy rainfall warning systems and ensuring better preparation in the face of increasing urban flood risks due to climate change.

Keywords: storm risk matrix; local ensemble prediction system; flood vulnerability; climate change

check for updates

Citation: Lee, S.; Choi, Y.; Ji, J.; Lee, E.; Yi, S.; Yi, J. Flood Vulnerability Assessment of an Urban Area: A Case Study in Seoul, South Korea. *Water* **2023**, *15*, 1979. https://doi.org/10.3390/w15111979

Academic Editor: Piotr Matczak

Received: 16 February 2023
Revised: 16 May 2023
Accepted: 22 May 2023
Published: 23 May 2023

1. Introduction

Climate change is altering weather patterns, leading to more extreme and frequent floods and droughts worldwide [1]. South Korea is not exempt from experiencing these climate change effects, particularly in terms of shifting rainfall patterns and intensity [2,3]. For instance, in 2020, the rainy season lasted 54 days, longer than the average duration in previous years, resulting in severe nationwide inundation damage. The frequency and scale of damage from heavy storms have been progressively increasing, with urban areas being relatively more vulnerable due to high population density and property concentration. Rapid urbanization in major cities and countries is among the key factors contributing to the heightened risk of flood damage [4,5].

Recent flooding in Seoul, South Korea's capital, underscores the city's vulnerability to heavy rainfall, causing casualties, and property damage, as well as revealing challenges within the city's sewer system [6]. Sewage backflow has been the main cause of road inundation near the Gangnam subway station and Gwanghwamun area over the past decade. In urban areas, inundation damage during storms results from rainfall exceeding the sewer network's design frequency. While river flooding was historically the primary cause of inundation damage, increasing impervious areas have become a major contributing factor.

In South Korea, regions prepare for and respond to flood damage based on special weather reports issued by the Korea Meteorological Administration (KMA) [7]. KMA issues storm watches or warnings if 3 h rainfall exceeds 60 or 90 mm, respectively. However, this criterion is identical nationwide, despite varying flood damage characteristics in densely populated districts such as Seoul, Busan, and Incheon, due to differing geographical conditions, meteorological factors, and local features. For instance, during a July 2016 storm event, Gangnam-Gu and Seocho-Gu experienced inundation damage, while Gwanak-Gu did not, despite having similar rainfall levels.

Given the different levels of flood damage in Seoul, there is a need to develop a rainfall standard for more localized heavy rainfall warnings, reflecting local meteorological and geographic characteristics. Rainfall standard refers to the levels at which warning levels can be issued based on rainfall amount, and the degree of rainfall can be classified as interest, caution, warning, or serious according to these criteria. Proper flood damage responses should incorporate both local characteristics and flood vulnerability, which refers to a community's susceptibility to flooding's negative impacts. Vulnerability depends on exposure to flood hazards and resilience or coping ability with those hazards.

Previous studies used flood vulnerability models and evaluation indicators to analyze vulnerability. The entropy and AHP methods, based on the Pressure-State-Response (PSR) model, are employed to analyze flood vulnerability [8,9]. Developed by the Organization for Economic Cooperation and Development (OECD), the PSR system is commonly used to assess flood vulnerability, along with the climate change vulnerability model established by the Intergovernmental Panel on Climate Change (IPCC) [10]. Among these methods, the AHP method produced reasonable results in calculating weights when sufficient data and various alternatives were available. However, results rarely have high reliability, as most cases need to verify the results after determining the alternatives [11]. Thus, there is an urgent need to develop a method to calculate weight with high reliability.

A climate change vulnerability assessment model is a tool employed to evaluate the potential impacts of climate change on a specific system or region. The PSR system, which comprises pressure, state, and response indices, evaluates event causes, effects, and damage reduction levels to determine vulnerability.

OECD's methods calculate regional flood risk indices by estimating the weight of each indicator. Alternative approaches to spatial flood vulnerability analysis include the Fuzzy Technique for Order Preference by Similarity to Ideal Solution (TOPSIS) and the restricted weighted-sum method [12]. IPCC's climate change vulnerability model is utilized in various studies for flood vulnerability analysis, regional flood damage assessment, and exploration of distribution characteristics through cluster analysis [13–15]. Other research has employed the Data Envelopment Analysis model, using population, lifespan, economic factors, and flood damage as input factors [16], or the AHP method to estimate and map urban flood vulnerability levels by calculating indicator weights [17]. Furthermore, efforts to develop flood vulnerability indices and flood mitigation planning continue based on flood vulnerability analysis [18–23].

KMA has examined past rainfall and designed rainfall to supplement current special weather warning standards and establish a new rainfall standard in South Korea [24,25]. Designed rainfall is an artificial or modified rainfall pattern used to simulate the effects of different precipitation types on a specific area or structure. Rainfall criteria determine the levels at which warning levels can be issued based on rainfall amount. Rainfall levels can be classified as interest, caution, warning, or serious according to these criteria. This includes adjusting the intensity, duration, and frequency of rainfall events to assess the potential impacts of extreme weather events or to design drainage and water management systems that can effectively handle various rainfall scenarios. The goal is to revise the special weather warning and disaster prevention indicators to differentiate the special weather warning standards by different districts. One study estimated the rainfall threshold by percentage to establish a rainfall standard [26]. Another study estimated the rainfall standard based on past flood damage and rainfall prediction data [27]. Other methods include physical-based or data-based modeling in establishing a rainfall standard and predicting urban flooding [28–30].

As we expect more extreme and frequent weather events, especially in urban areas such as Seoul, it is essential to have mitigation plans for flood damage. An imminent problem in Seoul during the rainy season is flood damage due to excessive rainfall that exceeds the designed capacity of drainage systems. The drainage system in Seoul was not initially designed to hold extreme floods, causing casualties and property losses. However, flood damages differ across the 25 districts inside Seoul during storm events.

To address this gap, this study's primary objective is to assess flood vulnerability, taking into account regional characteristics, and to establish a rainfall standard for predicting and reducing urban flood damage caused by frequent heavy storms in Seoul. The sub-objectives include the following: (a) estimating entropy weight, (b) evaluating flood vulnerability across 25 districts, (c) assessing regional flood vulnerability, (d) estimating a region-specific rainfall standard, (e) developing storm risk matrices using rainfall standards, (f) evaluating the conformity of a rainfall standard based on past flood events, and (g) developing a storm risk prediction technique using rainfall forecasting data.

The novelty of this study lies in addressing the limitations of current standards by developing a rainfall standard that incorporates flood vulnerability and local characteristics. These region-specific rainfall standards can provide valuable information, enabling better preparation for heavy rainfall events.

2. Study Area

South Korea covers a total area of 100,399 km^2, with mountains comprising two-thirds of the country. The nation experiences four distinct seasons: spring from March to May, summer from June to August, autumn from September to November, and winter from December to February. The rainy season typically occurs from July to September, with an average annual rainfall of about 1300 mm. South Korea has a total population of 51.81 million.

Seoul, the capital and largest metropolitan city, spans an area of 605.25 km^2 and is home to 9.9 million people (Table 1). The Han River, South Korea's longest river, flows east to west through the city and its surrounding mountains. The river roughly divides Seoul into the Gangbuk area (north of the Han River) and the Gangnam area (south of the Han River). The city comprises 25 districts ("Gu"), with 14 districts in the Gangbuk area and 11 districts in the Gangnam area (Figure 1).

Table 1. Description of characteristics of 25 districts.

Districts	Area (km^2)	Population	Financial Independence Rate
Gangnam	47.0	425,126	54.7
Gangdong	41.4	580,185	21.1
Gangbuk	39.5	539,231	52.3
Gangseo	35.4	523,037	15.8
Gwanak	33.9	667,960	37.6
Gwangjin	29.7	479,835	17.9
Guro	29.6	495,060	19.3
Geumcheon	24.6	459,970	26.3
Nowon	24.6	437,153	20.0
Dobong	24.5	379,480	36.0
Dongdaemun	23.9	149,384	47.0
Dongjak	23.8	371,890	31.6
Mapo	23.6	308,055	16.8
Seodaemun	21.9	230,040	39.3
Seocho	20.7	325,257	18.4
Seongdong	20.1	404,408	22.2
Seongbuk	18.5	394,702	17.5
Songpa	17.6	312,173	23.4
Yangcheon	17.4	454,251	25.2

Table 1. *Cont.*

Districts	Area (km^2)	Population	Financial Independence Rate
Yungdeungpo	17.1	346,682	26.2
Yongsan	16.9	293,556	32.7
Eunpyeong	16.4	391,220	26.4
Jongno	14.2	342,837	23.2
Jung	13.0	231,733	24.7
Jungnang	10.0	125,240	53.5

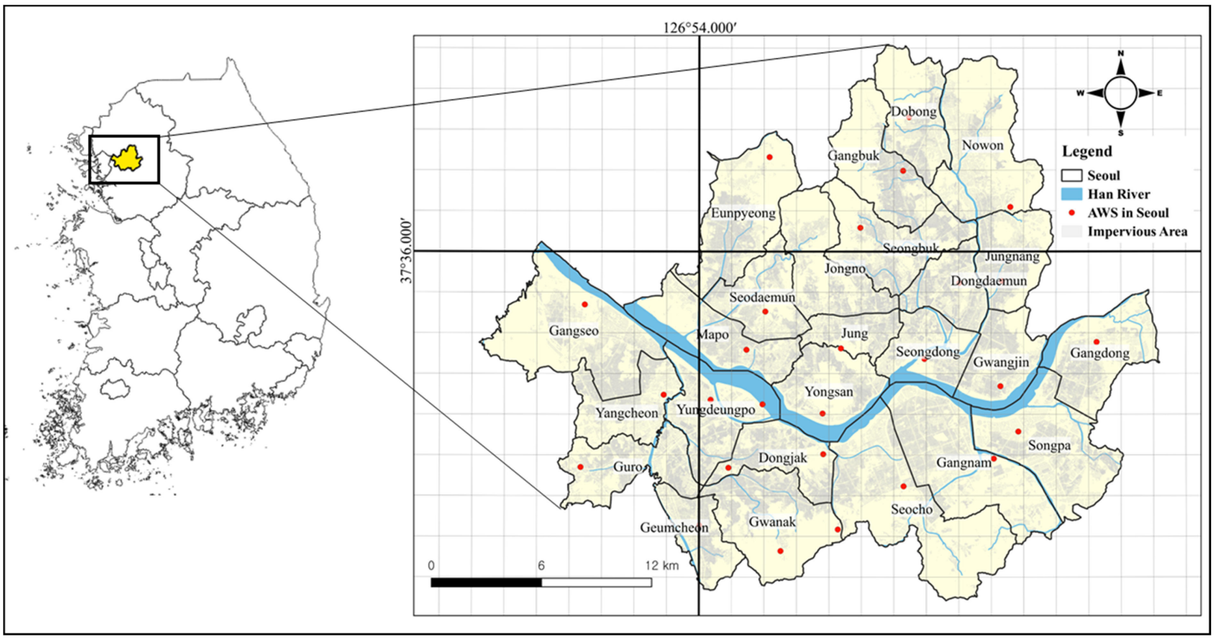

Figure 1. Over 60% of Seoul has undergone urbanization, and most regions have unfavorable geography for efficient rainwater drainage. The red points on the map represent the locations of automatic weather stations (AWS). Notably, there are no AWS installations in Jongno-Gu, while areas such as Yeongdeungpo-Gu have two or more. To compensate for this uneven distribution, the rainfall data was calculated using the areal average rainfall method based on the Thiessen polygon approach. The Han River, a significant geographic feature, flows through Seoul, further impacting the city's drainage dynamics.

Since the 1970s, Seoul has experienced rapid urbanization as it attracts migrants from across the country. The loss of natural ground is equivalent to the loss of permeable areas, while the gain of impervious surfaces and pavement leads to increased runoff. The growing impervious surface area in Seoul has resulted in inundation damage almost every year, as the terrain conditions are unfavorable for draining rainwater during storm events [31–34]. During heavy storms, Seoul faces casualties and property losses [35].

3. Methodology

Figure 2 displays the comprehensive workflow of this study. The study is divided into six steps: One, data collection and model selection (refer to Section 3.1); two, estimation of entropy weight based on different factors (refer to Section 3.2). The concept of entropy weight (EWM) is further detailed in Section 3.2; three, evaluation of flood vulnerability across the 25 districts in Seoul (refer to Section 3.3); four, estimation of district-specific rainfall standard (refer to Section 3.4); five, definition and development of a storm risk matrix using the estimated rainfall standard (refer to Section 3.5); six, creation of a storm risk prediction technique utilizing rainfall forecasting data (refer to Section 3.6).

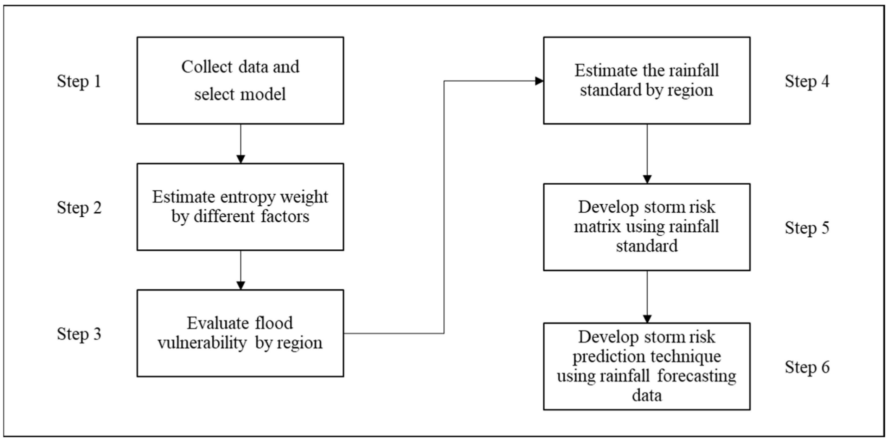

Figure 2. Workflow of this study.

3.1. Step 1: Collect Data and Select Model

We gather data to evaluate climate exposure, sensitivity, and adaptive capacity. Climate exposure refers to the extent to which a specific system or region is vulnerable to the impacts of climate change. Sensitivity is a factor that assesses how susceptible each district is to flood damage. Adaptive capacity refers to the ability to respond to floods and assesses disaster prevention characteristics. Section 3.1.1 addresses climate exposure and its associated sub-factors. Section 3.1.2 delves into sensitivity and its related sub-factors. Section 3.1.3 examines adaptive capacity and its sub-factors. Section 3.1.4 describes the process of model selection. Figure 3 illustrates climate exposure factors ((a–d) in blue), sensitivity factors ((e–j) in orange), and adaptive capacity factors ((k–o) in green).

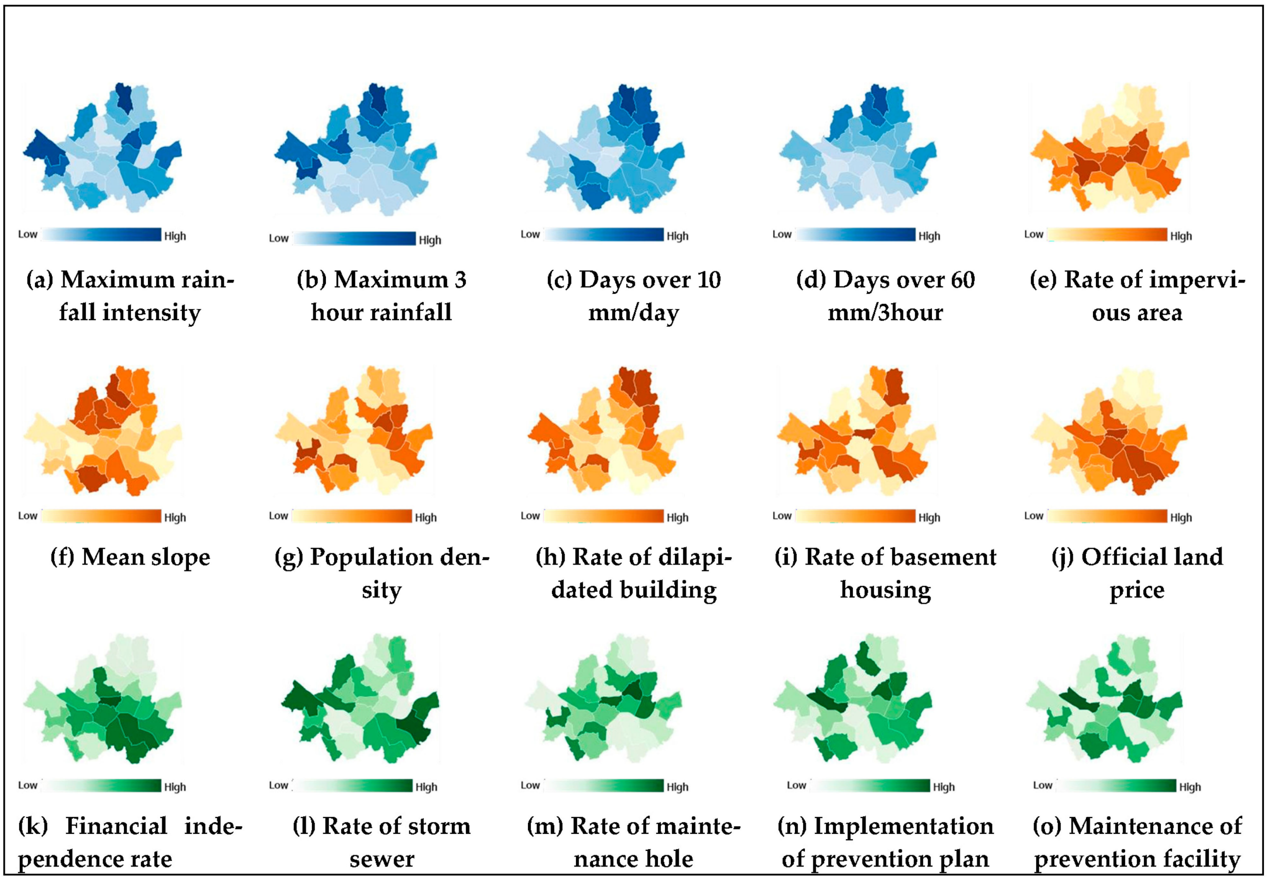

Figure 3. Data description showing the climate exposure factors (from (**a**–**d**) in blue), sensitivity (from (**e**–**j**) in orange), and adaptive capacity (from (**k**–**o**) in green).

3.1.1. Climate Exposure

Climate exposure measures how much a system is likely to be affected by variations in temperature, rainfall, sea level, extreme weather events, and other climate-related factors. The input data consists of 25 AWS in Seoul. Four sub-factors include maximum rainfall intensity, maximum 3 h rainfall, days with over 10 mm/day of rain, and days with over 60 mm/day of rain (Table 2). We select maximum rainfall intensity (mm/h) and maximum 3 h rainfall (mm/h) as sub-factors, as they determine the magnitude of rainfall intensity during a short period (Figure 3a,b). The days with at least 10 mm of rain contribute to the count of rainy days (Figure 3c). Days with over 10 mm/day indicate how frequently the region experiences rainfall. Days with over 60 mm/3 h evaluate the number of storm warning-issued days based on storm warning standards. Dobong-Gu has the highest number of days with over 60 mm/3 h, while Geumcheon-Gu has the lowest number (Figure 3d).

Table 2. A list of sub-factors for climate exposure.

Sub-Factor	Highest Value	Lowest Value
Maximum rainfall intensity (mm/h)	Dobong-Gu (67.5 mm/h)	Eunpyeong-Gu (32.4 mm/h)
Maximum 3 h rainfall (mm/3 h)	Dobong-Gu (104.1 mm/3 h)	Geumcheon-Gu (61.8 mm/3 h)
Days over 10 mm/day (days)	Dobong-Gu (160 days)	Jung-Gu (125 days)
Days over 60 mm/day (days)	Dobong-Gu (21 days)	Geumcheon-Gu (1 day)

We gather rainfall data from each station from the past five years (2016 to 2020) and estimate areal rainfall using Thiessen's Weighting Method. The Thiessen method calculates the areal average precipitation by connecting the perpendicular bisectors of the lines between observation points to form Thiessen polygons, determining the area ratio of each polygon within the watershed, and multiplying it by the precipitation at each observation point before summing them up. This method accounts for the distribution of precipitation based on the dominant area of each rain gauge observation point. In this study, we use data from 25 AWS sites within Seoul. However, there were no stations installed in Jongno-Gu. By using the Thiessen method, the areal average precipitation in Jongno-Gu can be calculated and compensated for using the surrounding observation points. We obtain climate exposure data from the KMA (https://www.weather.go.kr/w/index.do, accessed on 1 February 2021).

3.1.2. Sensitivity

Sub-factors used to evaluate sensitivity include the rate of impervious area, mean slope, population density, rate of dilapidated buildings, rate of basement housing, and official land prices (Table 3). We collect data on the rate of impervious areas from the Water Resources Management Information System (http://www.wamis.go.kr/, accessed on 1 February 2021). We gather digital elevation model data to calculate the mean slope using topography analysis in geographic information system spatial analysis. We obtain population density, rate of dilapidated buildings, rate of basement housing, and officially announced land prices from Statistics Korea (KOSTAT).

Table 3. A list of sub-factors for sensitivity.

Sub-Factor	Highest Value	Lowest Value
Rate of impervious area (%)	Yungdeungpo-Gu (96%)	Gangbuk-Gu (41%)
Mean slope (%)	Gangbuk-Gu (18%)	Yungdeungpo-Gu (2%)
Population density (1/km^2)	Yangcheon-Gu (26,321 people/km^2)	Jongno-Gu (6327 people/km^2)
Rate of dilapidated building (1/km^2)	Yangcheon-Gu (2664 count/km^2)	Gangseo-Gu (489 count/km^2)
Rate of basement building (1/km^2)	Jung-Gu (31 count/km^2)	Jongno-Gu (4/km^2)
Officially announce land price (won/km^2)	Gangnam-Gu (8,628,861 won/km^2)	Dobong-Gu (2,037,798 won/km^2)

Impervious surface area refers to surfaces that water cannot penetrate, such as asphalt roads, buildings, and artificial pavement. Areas with high impervious surface areas experience increased runoff due to the inability of rainwater to infiltrate the ground. Consequently, areas with high impervious surfaces are more vulnerable to flooding, leading to significant flood damage (Figure 3e). The mean slope is inversely proportional to sensitivity. Terrain with a lower mean slope is more vulnerable to rainwater drainage issues. According to previous studies, areas with lower average slopes are more likely to experience flood damage, such as that caused by river flooding [36]. Therefore, terrain with a lower mean slope is more vulnerable to rainwater drainage (Figure 3f).

Factors such as population density, rate of dilapidated buildings, rate of basement housing, and official land prices reflect the local characteristics of districts. Population density refers to the population of a specific area divided by the area's size. In the event of a flood, areas with higher populations are more likely to experience more extensive damage, such as human casualties, compared to other areas (Figure 3g). The rate of dilapidated buildings refers to the ratio of buildings over 30 years old per unit area. Dilapidated buildings are more likely to have poor disaster resilience, such as in the case of flooding, and may be at risk of collapse or other damage (Figure 3h). The rate of basement buildings refers to the proportion of buildings with basements per unit area. Areas with a high proportion of buildings with basements are more likely to experience flood damage because the presence of basements increases the likelihood of flooding (Figure 3i). Official land prices refer to the prices used as the taxation base for real estate assets such as land and buildings in each region. Areas with high standard land prices may result in significant property damage in the event of flooding (Figure 3j).

3.1.3. Adaptive Capacity

Adaptive capacity is inversely proportional to flood vulnerability. The sub-factors for adaptive capacity include the financial independence rate, rate of storm sewer occurrence, rate of maintenance hole occurrence, index for implementation of prevention plans, and index for prevention facilities (Table 4). Financial independence is an indicator of a local government's ability to secure income independently. It serves as a measure of a region's property value, and areas capable of allocating more funds to disaster preparedness are assessed as having a higher level of disaster preparedness (Figure 3k). The ratio of storm sewers and maintenance refers to the ratio of the length of sewer pipes and the number of manholes per unit area. Areas with more facilities for managing rainfall, such as sewer pipes and manholes, are evaluated as having a higher level of disaster preparedness (Figure 3m,n).

Table 4. A list of sub-factors for adaptive capacity.

Sub-Factor	Highest Value	Lowest Value
Rate of financial independence (%)	Seocho-Gu (54.9%)	Nowon-Gu (15.4%)
Rate of storm sewer (m/km^2)	Dongdaemun-Gu (3048 m/km^2)	Nowon-Gu (85 m/km^2)
Rate of maintenance hole (/km^2)	Jung-Gu (2342/km^2)	Seocho-Gu (674/km^2)
Index for prevention plan (-)	Mapo-Gu (1.01)	Guro-Gu (0.418)
Index for prevention facility (-)	Mapo-Gu (1.00)	Geumcheon-Gu (0.463)

Statistical data from drainage system maintenance plans serve as input data for adaptive capacity assessment. In 2017, the Ministry of the Interior and Safety calculated the local safety index using the index for prevention plans and the index for prevention facilities. The Local safety index, calculated by the Ministry of the Interior and Safety, assesses disaster risk factors, disaster prevention measures, facility inspections, maintenance, and 53 other indicators nationwide. The prevention plan refers to efforts to reduce the impact of natural disasters, with the Prevention Index calculated by considering 28 indicators such as the establishment of plans for river, stream, and sewage maintenance, and the inspection of disaster-prone areas (facilities). Additionally, the Prevention Facility Investment Index is calculated by considering 18 indicators such as the installation of sewage pipes and drainage pump stations related to the maintenance of natural disaster-prone areas and prevention facilities. We extract adaptive capacity data from the Ministry of the Interior and Safety (https://www.mois.go.kr/eng/a01/engMain.do accessed on 1 February 2021). Higher climate exposure and sensitivity, along with lower adaptive capacity, indicates that a district is more vulnerable to floods.

3.1.4. Model Selection

A climate change vulnerability assessment model is a tool employed to evaluate the potential impacts of climate change on a specific system or region [37]. These models utilize a variety of inputs, such as data on historical climate patterns, projections of future climate scenarios, and information on how different sectors of the economy and society may be affected by changes in temperature, precipitation, sea levels, and other climate-related variables. We apply the climate change vulnerability assessment model for flood vulnerability assessment by incorporating local flood damage-related factors, such as local climate, topography, and disaster prevention characteristics. The three main indices for flood vulnerability assessment are climate exposure, sensitivity, and adaptive capacity (Figure 4).

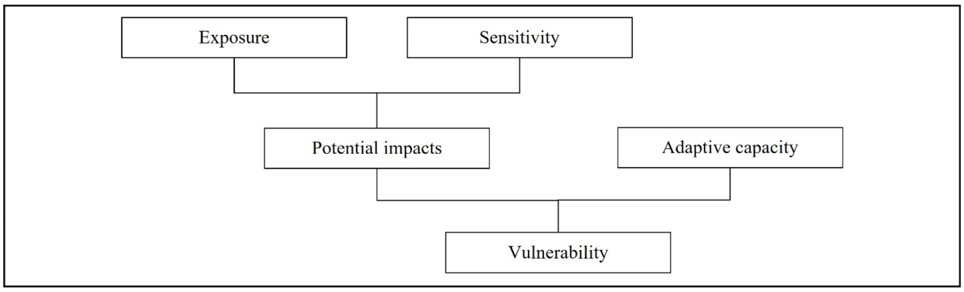

Figure 4. Climate change vulnerability assessment model for flood vulnerability assessment.

3.2. Step 2: Estimate Entropy Weight by Different Factors

Multi-criteria decision-making is a process that involves evaluating and prioritizing multiple alternatives based on various conflicting criteria. Some of the most used multi-criteria decision-making methods include AHP, TOPSIS, and EWM.

AHP is a technique for organizing and analyzing complex decisions; AHP breaks down the problem into a hierarchy of smaller, interrelated criteria. AHP is a highly intuitive and flexible method that allows decision-makers to easily incorporate their judgments and preferences through pairwise comparisons. However, AHP can be sensitive to inconsistencies in pairwise comparisons, which may lead to inaccurate results [38].

TOPSIS involves ranking alternatives based on their relative closeness to an ideal solution and distance from the worst solution. TOPSIS is relatively simple to understand and apply, and it considers both the positive and negative aspects of alternatives, offering a balanced evaluation. The method assumes that criteria are independent, which may not always be the case in real-world decision-making problems [39].

EWM is a decision-making tool used in multi-criteria decision analysis to determine the relative importance or weight of different criteria in a decision-making process [40]. The method is based on the concept of entropy, which is a measure of the degree of randomness or disorder in a system. In EWM, each criterion is assigned a weight based on its relative entropy value, which is calculated by comparing the performance scores of different alternatives against each criterion [41]. EWM assumes that higher entropy implies higher importance, which may not always hold true in practice [42,43].

We employ EWM to calculate the weights of sub-factors (Figure 5). EWM offers an objective approach for determining criterion weights based on the information content of each criterion. This reduces the reliance on subjective judgments and may lead to more reliable and unbiased results. The estimated weights illustrate the importance of sub-factors in calculating flood vulnerability [44].

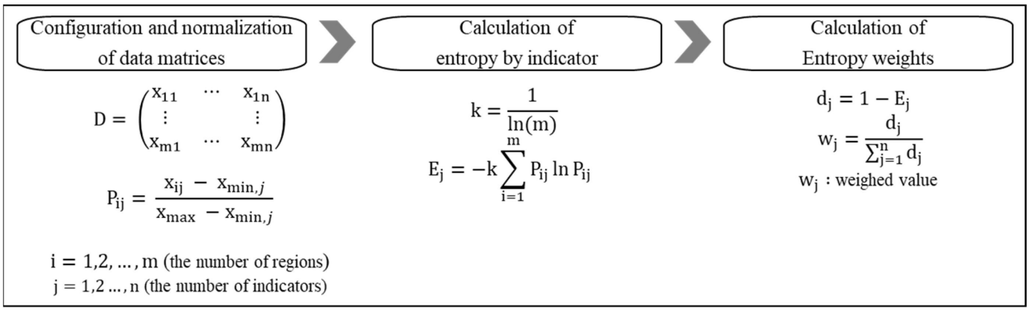

Figure 5. Workflow of calculating the entropy weights. To calculate the entropy weights, we configure and normalize data metrics and calculate the entropy by indicator.

The first step involves collecting the sub-factor data for each assessment factor and constructing a matrix. We normalize the data using the Min-Max method, which generates values between 0 and 1. Then, we apply the entropy weight values and constant to calculate the degree of diversity and weight (Table 5).

Table 5. Entropy weights calculated considering the variance of each sub-factor.

Sub-Factor	Entropy Weights
Maximum rainfall intensity (mm/h)	0.175
Maximum 3 h rainfall (mm/3 h)	0.255
Days over 10 mm/day (days)	0.261
Days over 60 mm/day (days)	0.309
Rate of impervious area (%)	0.134
Mean slope (%)	0.123
Population density (1/km^2)	0.200
Rate of dilapidated building (1/km^2)	0.196
Rate of basement building (1/km^2)	0.208
Officially announce land price (won/km^2)	0.138
Rate of financial independence (%)	0.168
Rate of storm sewer (m/km^2)	0.204
Rate of maintenance hole (/km^2)	0.243
Index for prevention plan (-)	0.201
Index for prevention facility (-)	0.185

3.3. Step 3: Evaluate Flood Vulnerability by Region

Various methods are considered for calculating flood vulnerability using indices of climate exposure, sensitivity, and adaptability, including simple average, weighted average, and Euclidean distance. The simple average method offers the advantage of calculating flood vulnerability mathematically by averaging each index, assuming equal importance of each factor. However, it is influenced by outliers in the data when calculating the average value [45]. Conversely, the weighted average method better reflects the data characteristics than the simple average method by assigning weights to each factor according to its importance. However, the subjective determination of weights makes it challenging to produce objective results [46]. By using the Euclidean distance method, researchers can calculate flood vulnerability by considering all evaluation factors and excluding subjective judgments through simple calculations. Therefore, we apply the Euclidean distance method, and the main input data are the results of climate exposure, sensitivity, and adaptive capacity for 25 districts using the EWM.

Euclidean distance is a measure of the distance between two points in Euclidean space [47]. In two-dimensional space, Euclidean distance is the straight-line distance between two points, as calculated using the Pythagorean theorem. In n-dimensional space, the Euclidean distance between two points is calculated using the square root of the sum of the squares of the differences between each coordinate (Figure 6). The Euclidean distance method is a common approach for quantitative analysis and cluster analysis of data [48]. The Ministry of Interior and Safety in South Korea applies the Euclidean distance method to calculate the local safety index. Unlike other approaches such as the simple average method, the Euclidean distance method can apply climate exposure, sensitivity, and adaptive capacity in assessing vulnerability. The origin (0, 0, 0) in a three-dimensional space composed of climate exposure, sensitivity, and 1-adaptive capacity is the safest area from floods. The flood vulnerability is the distance from the origin to the coordinates of the target area (climate exposure, sensitivity, 1-adaptive capacity). See Equation (1) for calculating flood vulnerability.

$$Flood\ vulnerability = \sqrt{(Climate\ Exposure)^2 + (Sensitivity)^2 + (1 - Adaptive\ capacity)^2)} \quad (1)$$

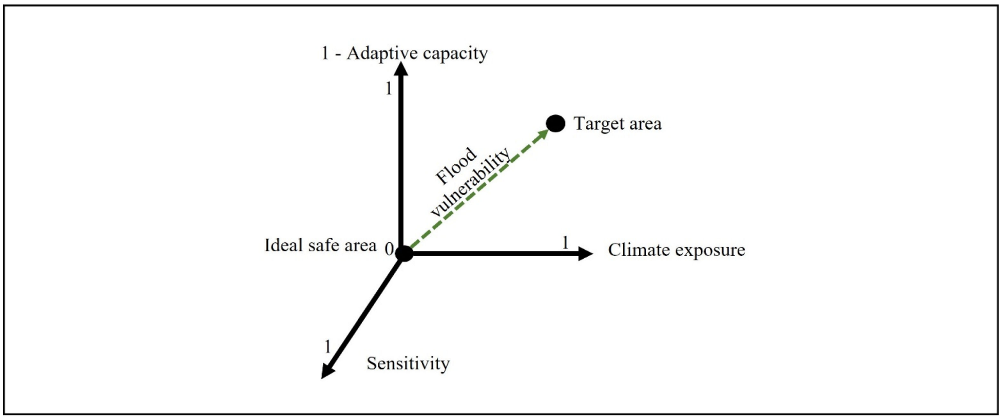

Figure 6. Calculating the flood vulnerability using Euclidean distance.

3.4. Step 4: Estimate the Rainfall Standard by Region

Rainfall standard designates threshold levels for issuing warnings based on the amount of precipitation, with classifications such as interest, caution, warning, or serious. The primary input for establishing these standards is the historical rainfall data from storm events in Seoul, spanning from 2010 to 2020. We analyze flood vulnerability and probability of rainfall by incorporating regional characteristics from the 25 districts in Seoul. The probability of rainfall is estimated by applying probability distribution models such as Gumbel or generalized extreme value to the rainfall data, selecting the optimal distribution type through parameter application and suitability testing, and then calculating the probability through frequency analysis.

We define the rainfall ratio as the ratio of damaging rainfall to probability of rainfall. Damaging rainfall refers to the amount of precipitation that causes harm to infrastructure, property, and ecosystems, potentially leading to floods, landslides, and erosion, which pose significant threats to public safety and well-being. In the context of climate change, concerns arise about the increasing frequency and intensity of damaging rainfall events due to changes in temperature and precipitation patterns.

Damaging rainfall represents the amount of precipitation responsible for flood damage and casualties. We calculate the average rainfall ratio for four flood damage levels and use these values to establish rainfall standard. To compute damaging rainfall, we utilize historical rainfall data from flood events between 2010 and 2020. We then employ the flood impact table developed by Choi et al. to describe flood damage levels from 1 to 4, based on the severity of flood damage [49] (Table 6). Level 1 represents minimal flood damage, while level 4 signifies the most severe flood damage experienced in South Korea.

Table 6. Description of flood damage for four levels.

Level	Description of Flood Damage
Level 1	Clothing may get wet if the rainfall lasts for a long time Small puddles form in the ground Buildings may need inspection Some assets are flooded
Level 2	Clothing may get wet by walking around Big puddles form in the ground Farmlands may get damaged by local flooding
Level 3	Clothing gets wet with an umbrella Inundation occurs Small streams overflow Roads are blocked due to flooding Buildings and structures may get damaged
Level 4	Heavy rain blocks the view Large areas are flooded Water overflows from maintenance holes Cars may get inundated Buildings and structures may collapse

To test the suitability of our proposed rainfall standard, we predict flood risk using past flood damage events as input data for each district, evaluating their appropriateness. We use flood damage data from the last five years (2016 to 2020). We chose this recent timeframe because over 200 houses in the Gangbuk area were flooded in 2018. Moreover, in 2020, Seoul experienced its longest rainy season, during which Dobong-Gu and Nowon-Gu suffered inundation damage, especially due to flooding from the Jungnang stream.

3.5. Step 5: Develop Storm Risk Matrix Using Rainfall Standard

The storm risk matrix, as illustrated in Figure 7, is composed of rainfall criteria on the x-axis and the likelihood of high-impact rainfall on the y-axis. Four distinct colors within the matrix indicate storm risk levels, including concern, caution, alert, and emergency. We apply the concept of impact forecasting to modify the UK matrix and develop our storm risk matrix.

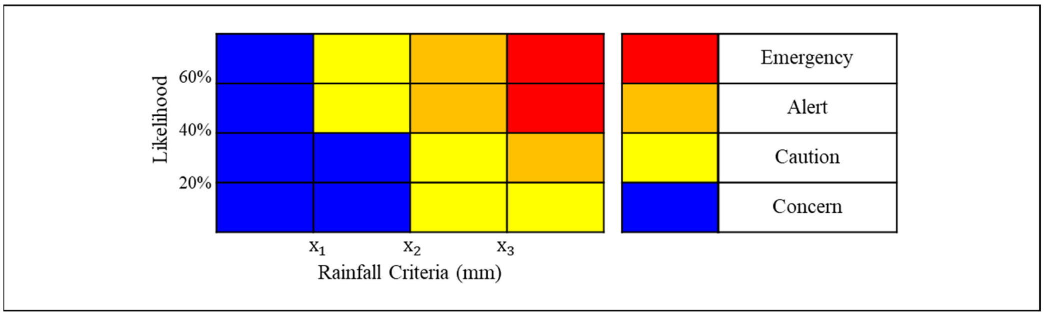

Figure 7. Storm risk matrix in South Korea. The storm risk levels have four levels including concern (blue), caution (yellow), alert (orange), and emergency (red).

The UK developed a matrix for five meteorological events: rain, wind, snow, ice, and fog [50]. This matrix addresses high-impact weather by representing the degree of impact on the *x*-axis and the likelihood of high-impact weather on the *y*-axis (Figure 8). Based on this matrix, the UK Meteorological Office issues special weather warnings up to five days in advance.

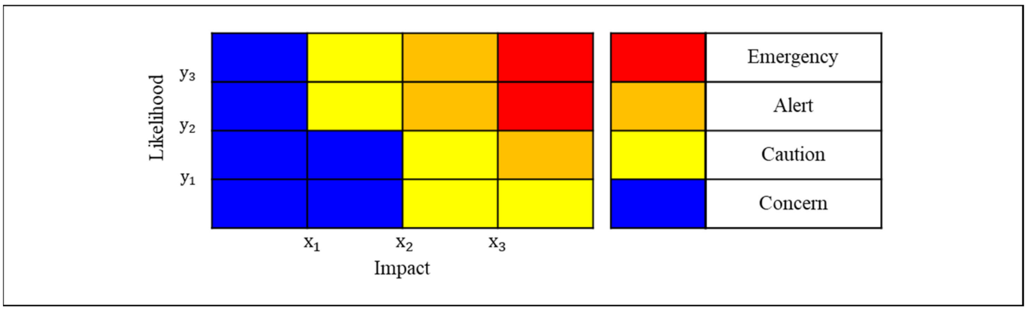

Figure 8. Natural hazard risk matrix in UK. The storm risk levels have four levels including concern (blue), caution (yellow), alert (orange), and emergency (red).

The primary inputs for our matrix are probability of rainfall and rainfall damage data from historical storm events, which include hazard intensity, vulnerability, and exposure. Probability of rainfall is estimated by applying probability distribution models such as Gumbel or generalized extreme value to rainfall data, selecting the optimal distribution type through parameter application and suitability testing, and then calculating the probability through frequency analysis. For the likelihood (y-axis), we adopt 20%, 40%, and 60% standards based on the high-impact weather of the UK matrix. After constructing the matrix according to the x- and y-axes, we categorize storm risk levels into concern (blue), caution (yellow), alert (orange), and emergency (red). The concern level indicates that people should be aware of potential hazards, while the caution level suggests that people should remain vigilant for possible hazards. The alert level requires preparation, and the emergency level calls for precautionary action [51].

Frequency analysis serves as the primary method for calculating probability of rainfall. We apply rainfall data to the probability distribution model to estimate probability of rainfall. To incorporate the sewer network and small rivers, we use the 5-year frequency (the design frequency of branch pipes), 10-year frequency (the design frequency of main pipes), and 30-year frequency (the design frequency of small rivers) when calculating probability of rainfall. We also use 3 h duration rainfall as input data, as Seoul experiences more frequent heavy rainfall events within shorter durations. The 3 h duration rainfall refers to the total amount of precipitation occurring during a continuous 3 h period.

3.6. Step 6: Develop Storm Risk Prediction Technique Using Rainfall Forecasting Data

Numerical weather prediction models are available in various forms. One such model is the European Centre for Medium-Range Weather Forecasts model, which applies high-resolution data and diverse physical processes to generate predictions. This model is considered the most accurate in the world; however, its complex calculations and relatively slow processing time result in slower prediction speeds [52]. Another model is the Global Forecasting System model, developed by the US National Weather Service and used worldwide. This model reflects large-scale atmospheric motion and physical processes, yielding a wide range of predictions. However, its prediction accuracy is comparatively low, particularly in precipitation forecasting [53].

Local Ensemble Prediction System (LENS) is a numerical weather prediction system providing high-resolution, short-term weather forecasts for specific regions or locations [54]. LENS employs an ensemble approach, which involves running multiple weather model simulations with slightly different initial conditions or parameters. These simulations allow the system to offer a range of possible weather outcomes and estimates of the likelihood of each outcome, enabling forecasters to better comprehend potential weather scenarios and make more informed decisions about the timing and impact of weather events.

LENS is tailored for local-scale use and can produce forecasts with a resolution of just a few kilometers. This makes it a valuable tool for applications such as transportation planning, emergency management, and agriculture, where accurate and timely weather information is crucial. Consequently, we utilize LENS with a spatial resolution of 3 km and propose a flood risk prediction method (Figure 9). We opt for LENS because the KMA has employed this system since 2015 to predict extreme weather events and provide earlier warnings.

LENS data in Korea comprises a control member and 12 perturbation members, which simultaneously offer ensemble and probability values for predicting weather factors [55]. KMA uses the Global Ensemble Prediction System and LENS data to provide probabilistic predictions for up to 72 h, at hourly increments from 0:00 a.m. to 12:00 p.m. In Korean Standard Time, LENS data becomes available at 4:00 a.m. and 4:00 p.m. Since 2018, the resolution of LENS data has improved from 3 km to 2.2 km [56]. We apply LENS data (from 2016 and 2017) and rainfall standard to evaluate flood risk prediction results.

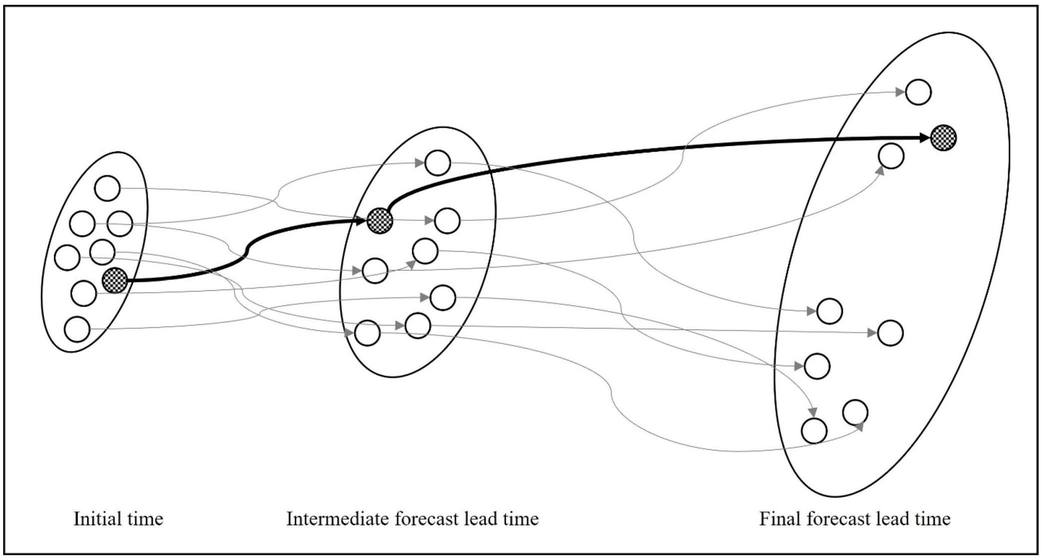

Figure 9. Illustration of ensemble prediction [57].

4. Results

4.1. Flood Vulnerability Assessment

The three primary indices for flood vulnerability assessment are climate exposure, sensitivity, and adaptive capacity (Figure 10). Dobong-Gu exhibited the highest climate exposure (1.00), while Jung-Gu displayed the lowest (0.153). Yangcheon-Gu demonstrated the highest sensitivity (0.673), whereas Jongno-Gu showed the lowest sensitivity (0.113). Mapo-Gu had the highest adaptive capacity (0.659), while Nowon-Gu possessed the lowest adaptive capacity (0.185). Dobong-Gu recorded the highest flood vulnerability (1.37), and Jongno-Gu registered the lowest flood vulnerability (0.609).

4.2. Rainfall Assessment

4.2.1. Rainfall Standard

We categorized the probability of rainfall into three levels: level 2 (5-year frequency), level 3 (10-year frequency), and level 4 (30-year frequency) (Table 7). Level 1, based on 5 mm, requires attention, but the probability of flooding during the storm remains low. Levels 2, 3, and 4 represent a rainfall standard that redistributed the probability of rainfall for each district according to flood vulnerability and the rainfall ratio (Figure 11). We employed the results from the local-specific rainfall standard to establish a storm risk matrix for forecasting storm risk (Table 8). The outcomes demonstrated that the rainfall standard for Levels 2 and 4 was similar to 60 mm/3 h (heavy rain advisory) and 90 mm/3 h (heavy rain warning) standards.

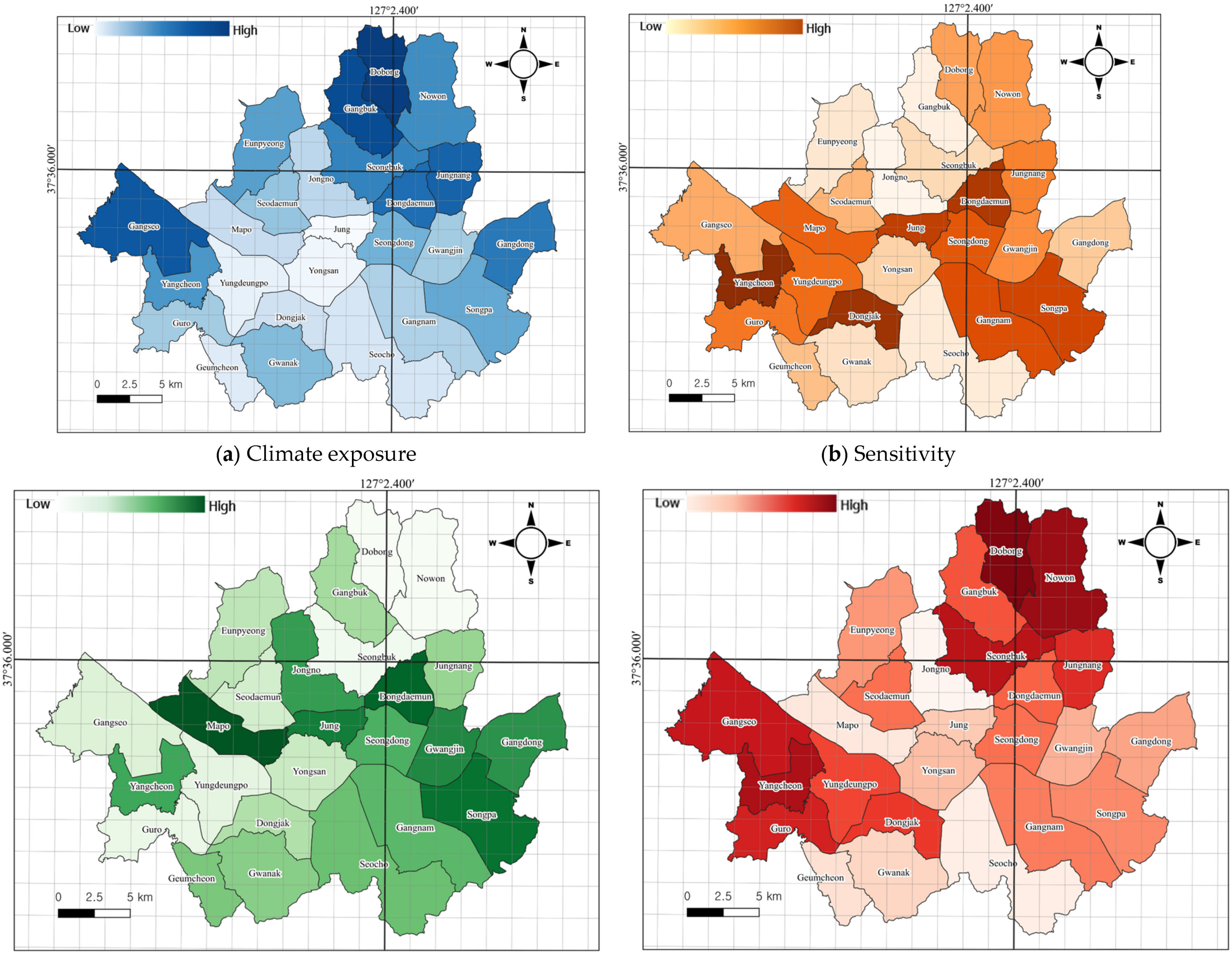

(**a**) Climate exposure (**b**) Sensitivity

(**c**) Adaptive capacity (**d**) Flood vulnerability

Figure 10. Calculated factors (climate exposure, sensitivity, and adaptive capacity) for assessing flood vulnerability using the entropy method.

Table 7. Calculated rainfall ratio for Levels 2, 3, and 4, and their averages.

Level	Damaging Rainfall (DR)	Probability of Rainfall (PR)	Rainfall Ratio (DR/PR)	Corrected PR
	mm/3 h	mm/3 h	-	mm/3 h
2	39.0	116.7	0.334	56.6
3	71.0	138.4	0.513	67.1
4	104.0	171.3	0.607	83.0
Average	-	-	0.485	68.9

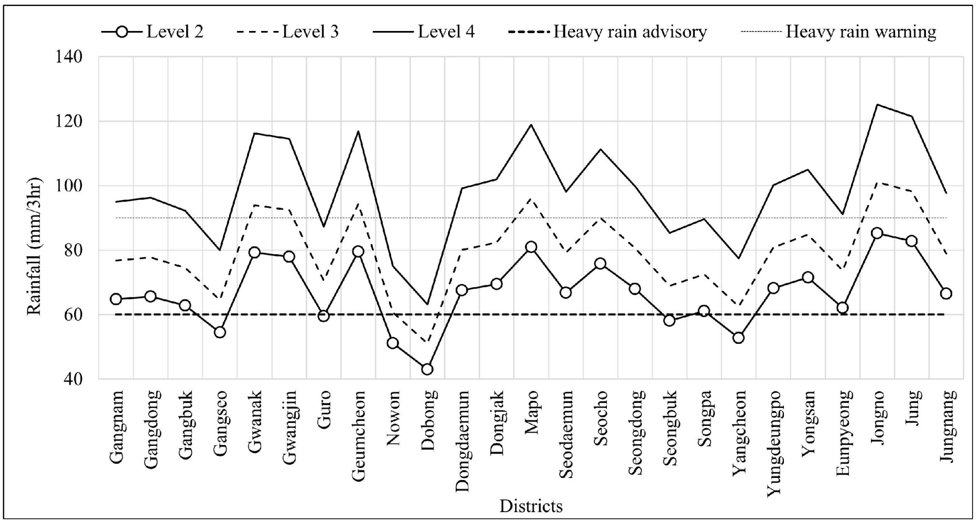

Figure 11. Rainfall standard for 25 districts in Seoul.

Table 8. Results of the *x*-axis value of the Storm Risk Matrix. The *y*-axis is the same for all regions, and the *x*-axis can be used to construct a Storm Risk Matrix by applying rainfall criteria calculated based on flood vulnerability.

Administrative Districts	**Level 1**	**Level 2**	**Level 3**	**Level 4**
	mm/3 h			
Gangnam-Gu	5.00	64.73	76.76	95.01
Gangdong-Gu	5.00	65.59	77.78	96.27
Gangbuk-Gu	5.00	62.80	74.48	92.18
Gangseo-Gu	5.00	54.47	64.60	79.95
Gwanak-Gu	5.00	79.19	93.92	116.25
Gwangjin-Gu	5.00	77.97	92.46	114.44
Guro-Gu	5.00	59.49	70.55	87.32
Geumcheon-Gu	5.00	79.57	94.37	116.80
Nowon-Gu	5.00	51.16	60.67	75.10
Dobong-Gu	5.00	43.04	51.05	63.18
Dongdaemun-Gu	5.00	67.56	80.13	99.18
Dongjak-Gu	5.00	69.46	82.37	101.96
Mapo-Gu	5.00	80.99	96.05	118.88
Seodaemun-Gu	5.00	66.85	79.28	98.13
Seocho-Gu	5.00	75.82	89.92	111.30
Seongdong-Gu	5.00	67.98	80.62	99.78
Seongbuk-Gu	5.00	58.11	68.92	85.30
Songpa-Gu	5.00	61.08	72.43	89.65
Yangcheon-Gu	5.00	52.73	62.53	77.40
Yungdeungpo-Gu	5.00	68.18	80.86	100.09
Yongsan-Gu	5.00	71.51	84.81	104.96
Eunpyeong-Gu	5.00	62.12	73.67	91.18
Jongno-Gu	5.00	85.26	101.12	125.16
Jung-Gu	5.00	82.77	98.16	121.50
Jungnang-Gu	5.00	66.51	78.88	97.63

We set the threshold for the first level of rainfall criteria at 5 mm/3 h, indicating rainfall unlikely to cause damage if it persists for 3 h. Additionally, the second and fourth levels of rainfall criteria were determined based on the "heavy rain advisory" and "heavy rain warning" criteria, respectively. This allows for issuing risk levels tailored to each region, considering regional characteristics such as existing heavy rain advisory criteria. The rainfall criteria calculated in this study provide a level of accuracy comparable to heavy rain advisory criteria.

The damage description indicates the magnitude of the damage. Since 2010, the primary causes of flood damages have been inundation and maintenance hole backflow. In 2011, a landslide occurred on Mount Umyeon. The area faced a high risk of inundation due to large puddles when more than 39 mm of rainfall persisted for over 3 h (Table 9). The area might experience inundation damage to roads and houses once it receives more than 71 mm of rainfall. Maintenance hole backflow may occur when the area experiences more than 104 mm of rainfall. We utilized storm events from 28 August 2018 and 6 August 2020 to evaluate the suitability of the established rainfall standard (Table 10). Seoul witnessed more than 80 mm of rainfall during these two storm events. During this period, the rainfall levels were compared with the flood damage levels according to the flood damage chart. In the first period, Seongbuk-gu, Eunpyeong-gu, Dobong-gu, and Nowon-gu experienced values at the same level, unlike other regions. In the second period, the rainfall level was lower than the damage level.

Table 9. Historical flood damages in Seoul from 2010 to 2020.

Start Date	End Date	Rainfall (mm/3 h)	Level	Damage Description
13 August 2010	18 August 2010	39	2	Big puddle in the ground
21 Jun 2011	3 July 2011	65	2	Big puddle in the ground
7 July 2011	16 July 2011	54	2	Big puddle in the ground
13 July 2012	13 July 2012	71	3	Inundation
5 July 2012	6 July 2012	95	3	Inundation
11 July 2013	15 July 2013	99	3	Inundation
1 July 2016	7 July 2016	85	3	Inundation
2 July 2017	11 July 2017	93	3	Breast wall collapse
21 September 2010	22 September 2010	174	4	Inundation
				Water overflows from maintenance holes
				Inundation
26 July 2011	29 July 2011	125	4	Landside on Woomyeon mountain
				Water overflows from maintenance holes
14 August 2012	16 August 2012	112	4	Inundation
				Water overflows from maintenance holes
22 July 2013	23 July 2013	130	4	Inundation
				Water overflows from maintenance holes
26 August 2018	1 September 2018	116	4	Inundation
				Water overflows from maintenance holes
28 July 2020	11 August 2020	104	4	Inundation
				Overflow from small streams

Table 10. Calculated factors (climate exposure, sensitivity, adaptive capacity) for assessing the flood vulnerability using the entropy method.

Event	District	Level		Damage Description
		Rainfall	Damage	
	Gangnam-Gu	1	2	Inundation
	Gangdong-Gu	1	2	Inundation
	Dongdaemun-Gu	1	2	Inundation
	Mapo-Gu	1	2	Inundation

Table 10. *Cont.*

Event	District	Level		Damage Description
		Rainfall	Damage	
28 August 2018	Seodaemun-Gu	1	2	Inundation
	Yangcheon-Gu	1	2	Inundation
	Seongbuk-Gu	2	2	Inundation
	Eunpyeong-Gu	2	2	Inundation
	Gangseo-Gu	3	2	Inundation
	Gangbuk-Gu	4	2	Inundation
	Nowon-Gu	4	4	Inundation, stream overflow in Jungnang River
	Dobong-Gu	4	4	Inundation, stream overflow in Jungnang River
6 August 2020	Gwanak-Gu	1	1	Blackout
	Gangbuk-Gu	1	2	Inundation
	Mapo-Gu	1	2	Inundation
	Seongbuk-Gu	1	2	Inundation
	Dobong-Gu	3	4	Inundation, stream overflow in Jungnang River

4.2.2. Storm Risk Prediction

We utilized six LENS datasets from 2016 (Table 11) and 2017 (Table 12), with the maximum value among the 12 perturbation members serving as the primary input. We compared flood risk outcomes for the storm events of 5 July 2016 and 23 July 2017 using observed rainfall and LENS data (Table 13).

Table 11. Calculated predicted flood risk level using the developed rainfall standard and storm risk levels based on LENS for the historical storm event (from 3 July 2016 to 5 July 2016).

District		Mapo	Nowon	Dobong	Jung	Jongno	Eunpyeong
Flood risk for observed rainfall		Yellow	Red	Red	Yellow	Yellow	Yellow
3 July 2016	4:00 a.m.	Blue	Yellow	Orange	Yellow	Blue	Yellow
	4:00 p.m.	Blue	Orange	Red	Yellow	Blue	Blue
4 July 2016	4:00 a.m.	Blue	Orange	Orange	Blue	Blue	Yellow
	4:00 p.m.	Yellow	Orange	Orange	Orange	Yellow	Blue
5 July 2016	4:00 a.m.	Blue	Yellow	Yellow	Yellow	Blue	Yellow
	4:00 p.m.	Blue	Blue	Blue	Blue	Blue	Blue

Table 12. Calculated predicted flood risk level using the developed rainfall standard and storm risk levels based on LENS for the historical storm event (from 21 July 2017 to 23 July 2017).

District		Nowon	Dobong	Jongno	Gangseo
Flood risk for observed rainfall		Red	Red	Yellow	Yellow
21 July 2017	4:00 a.m.	Blue	Blue	Blue	Blue
	4:00 p.m.	Red	Red	Orange	Blue
22 July 2017	4:00 a.m.	Blue	Blue	-	-
	4:00 p.m.	Orange	Blue	Blue	Yellow
23 July 2017	4:00 a.m.	Orange	Yellow	Blue	Blue
	4:00 p.m.	Blue	Blue	-	Blue

Table 13. Comparison of the flood risk for results through the storm events of 5 July 2016, and 23 July 2017.

Division	5 July 2016		23 July 2017	
	Flood Risk		Flood Risk	
	Observed Rainfall	LENS	Observed Rainfall	LENS
Mapo	Yellow	Yellow	-	-
Nowon	Red	Orange	Red	Red
Dobong	Red	Red	Red	Red
Jung	Yellow	Orange	-	-
Jongno	Yellow	Yellow	Yellow	Orange
Eunpyeong	Yellow	Yellow	-	-
Gangseo	-	-	Yellow	Yellow

5. Discussions and Conclusions

Dobong-Gu experienced the most rainfall in a short period, as this area had the highest maximum rainfall intensity and a maximum of 3 h of rainfall. Dobong-Gu also had the most days with over 100 mm/day and 60 mm/3 h of rainfall, indicating the highest climate exposure. In contrast, Yangcheon-Gu had the highest population density and dilapidated buildings, making it more likely to experience casualties and property damage. Jongno-Gu, with the lowest population density and rate of basement housing, was the least vulnerable to floods, while Mapo-Gu exhibited the highest adaptive capacity due to its comprehensive prevention plan and facilities.

Nowon-Gu and Dobong-Gu had the lowest rate of storm sewer infrastructure because of their mountainous geographic features. Dobong-Gu had the highest climate exposure (1.00) and the lowest adaptive capacity (0.185), making it the most flood-vulnerable. Conversely, Jongno-Gu had the lowest flood vulnerability (0.113) and a high adaptive capacity (0.961), indicating greater safety from flood damage. Our approach, which considers various regional characteristics such as climate, topography, and disaster management measures, can be useful for determining regional rainfall criteria and developing region-specific flood prevention measures.

During the two storm events in 2016 and 2017, Seoul experienced more than 70 mm of rainfall. KMA issued a special weather warning for the storm only a day in advance, but the city still suffered extensive flood damage. Our results, utilizing LENS data and the storm risk matrix, indicate that flood risk can be predicted up to three days in advance, enabling KMA to issue warnings earlier.

In our calculations, we used rainfall data from AWS for each region, and area-average rainfall was obtained through the Thiessen method. The accuracy of storm risk prediction using LENS data was somewhat lower in some areas, likely due to uncertainties in rainfall prediction data and data collection limitations. Flood damage data may be influenced by factors other than rainfall, such as other water systems, meteorological factors, and human factors. Improving the accuracy of LENS data and conducting a detailed analysis of flood damage causes could enhance flood risk assessment accuracy.

In this study, we assessed flood vulnerability for the local characteristics of the 25 districts in Seoul by incorporating local features. We also established a rainfall standard and a storm risk matrix based on the flood vulnerability for each district. To do so, we proposed a flood risk prediction method using LENS data. We selected 15 sub-factors of flood vulnerability, considering climate exposure, sensitivity, and adaptive capacity based on the IPCC's climate change vulnerability model. We calculated each district's flood vulnerability using entropy weight and Euclidean distance with the chosen sub-factors.

Seoul's northern and western areas, which are frequently exposed to high-intensity rainfall, have high climate exposure. These regions also have low adaptive capacity due to a lack of rainwater reduction facilities, resulting in high flood vulnerability. We constructed a storm risk matrix by calculating a rainfall standard. Although evaluating the suitability of the storm risk matrix using selected flood damage events differed from actual flood damage, we could predict flood risk three days in advance by applying LENS data to the storm risk matrix.

The predicted flood risk, based on the suitability of the rainfall standard for the 25 districts, was somewhat lower than the actual flood damage. This may be because we only considered factors other than rainfall when establishing a rainfall standard. Future studies could consider other hydrological and meteorological factors, such as flood volume, wind speed, or stormwater pump failures and building deterioration indexes. Actual flood damage can result from factors beyond rainfall, such as meteorological elements and human factors, despite being recorded as damages caused by rainfall in reports. By conducting a detailed cause analysis of the collected flood damage data, it is possible to construct a more effective flood risk matrix that accounts for the direct damage caused by rainfall.

One limitation of this study is the uncertainty in rainfall prediction data. Overcoming this limitation could involve developing a more accurate rainfall standard and a storm risk matrix by analyzing the causes of flood damage data used in this study. The innovative aspect of our research is addressing the current lack of adequate standards by developing storm risk criteria that incorporate flood vulnerability while considering local features. The resulting rainfall standard provides region-specific information, enabling more effective preparation for intense rainfall events and offering potential applicability to other case studies lacking tailored storm risk guidelines.

Author Contributions: Conceptualization, S.L., Y.C. and J.Y.; Data curation, S.L.; Formal analysis, S.L.; Funding acquisition, S.L., Y.C. and J.Y.; Investigation, S.L. and J.Y.; Methodology, S.L. and J.Y.; Project administration, S.L. and J.Y.; Resources, S.L., Y.C., J.J., E.L., S.Y. and J.Y.; Supervision, J.Y.; Validation, S.L.; Visualization, S.L. and S.Y.; Writing—original draft, S.L., S.Y. and J.Y.; Writing—review and editing, S.Y. and J.Y. All authors have read and agreed to the published version of the manuscript.

Funding: This work was supported by Korea Environment Industry & Technology Institute (KEITI) through Water Management Research Program, funded by Korea Ministry of Environment (MOE) (127569).

Data Availability Statement: Data and materials are available from the corresponding author upon request.

Conflicts of Interest: The authors declare no conflict of interest.

References

1. Omar, S.M.A.; Ariffin, W.N.H.W.; Sidek, L.M.; Basri, H.; Khambali, M.H.M.; Ahmed, A.N. Hydrological Analysis of Batu Dam, Malaysia in the Urban Area: Flood and Failure Analysis Preparing for Climate Change. *Int. J. Environ. Res. Public Health* **2022**, *19*, 16530. [CrossRef] [PubMed]
2. Kim, Y.T.; Park, M.; Kwon, H.H. Spatio-Temporal Summer Rainfall Pattern in 2020 from a Rainfall Frequency Perspective. *J. Korea Soc. Disaster Secur.* **2020**, *13*, 93–104.
3. Seo, K.; Lee, J. *White Paper of Changma*; Korean Meteorological Administration: Seoul, Republic of Korea, 2011.
4. Hammond, M.; Chen, A.; Djordjević, S.; Butler, D.; Mark, O. Urban flood impact assessment: A state-of-the-art review. *Urban Water J.* **2013**, *12*, 14–29. [CrossRef]
5. Waghwala, R.K.; Agnihotri, P. Flood risk assessment and resilience strategies for flood risk management: A case study of Surat City. *Int. J. Disaster Risk Reduct.* **2019**, *40*, 101155. [CrossRef]
6. Lee, S. *Flood Damage Situation*; Ministry of Environment: Sejong, Republic of Korea, 2018.
7. Song, Y.; Lim, C.; Joo, J.; Park, M. A Study on Heavy Rain Forecast Evaluation and Improvement Method. *J. Korean Soc. Hazard Mitig.* **2016**, *16*, 113–121. [CrossRef]
8. Song, J.H.; Kim, S.; Park, M.J.; Choi, H.I. Estimation of Flood Risk Index for the Nakdong River Watershed. *J. Korea Water Resour. Assoc.* **2013**, *46*, 35–45. [CrossRef]
9. Hwang, N.; Park, H.; Chung, G. Flood vulnerability analysis in Seoul, Korea. *J. Korea Water Resour. Assoc.* **2019**, *52*, 729–742.
10. Organization for Economic Cooperation and Development (OECD). *Environmental Indicators*; OECD: Paris, France, 1991.
11. Kim, W.Y.; Kim, D.H.; Choi, Y.C. A Study on application limitation of AHP priority vector with Expert measurement. *J. Korean Soc. Aviat. Aeronaut.* **2010**, *18*, 92–98.
12. Kim, Y.-K.; Chung, E.-S.; Lee, K.-S. Fuzzy TOPSIS Approach to Flood Vulnerability Assessment in Korea. *J. Korea Water Resour. Assoc.* **2012**, *45*, 901–913. [CrossRef]
13. Kim, J.; Sung, H.; Choi, G. Spatial Patterns of Urban Flood Vulnerability in Seoul. *J. Korean Assoc. Reg. Geogr.* **2013**, *9*, 615–626.

14. Tian, J.; Zeng, S.; Zeng, J.; Jiang, F. Assessment of Supply and Demand of Regional Flood Regulation Ecosystem Services and Zoning Management in Response to Flood Disasters: A Case Study of Fujian Delta. *Int. J. Environ. Res. Public Health* **2022**, *20*, 589. [CrossRef] [PubMed]
15. Shin, H.; Choi, Y.; Yi, J. Analysis of the Local Characteristics of Flood Damage Vulnerability in an Urban Area: The Han River Basin. *J. Korean Soc. Hazard Mitig.* **2019**, *19*, 293–303. [CrossRef]
16. Huang, D.; Zhang, R.; Huo, Z.; Mao, F.; Youhao, E.; Zheng, W. An assessment of multidimensional flood vulnerability at the provincial scale in China based on the DEA method. *Nat. Hazards* **2012**, *64*, 1575–1586. [CrossRef]
17. Ouma, Y.O.; Tateishi, R. Urban Flood Vulnerability and Risk Mapping Using Integrated Multi-Parametric AHP and GIS: Methodological Overview and Case Study Assessment. *Water* **2014**, *6*, 1515–1545. [CrossRef]
18. Nasiri, H.; Shahmohammadi-Kalalagh, S. Flood vulnerability index as a knowledge base for flood risk assessment in urban area. *J. Nov. Appl. Sci.* **2013**, *2*, 266–269.
19. Ologunorisa, T.E. An Assessment of Flood Vulnerability Zones in the Niger Delta, Nigeria. *Int. J. Environ. Stud.* **2004**, *61*, 31–38. [CrossRef]
20. UNDP (United Nations Development Program). *Reducing Disaster Risk: A Challenge for Development*; United Nations Development Program: New York, NY, USA, 2004.
21. Merabtene, T.; Yoshitani, J.; Kuribayashi, D.D. Managing Flood and Water-Related Risks: A Challenge for the Future I Am Working about 'Modeling Relationship Rainfull-Runoff' View Project Wastewater Treatment Modeling and Optimisation in Actvated Sludge Plantss View Projectwide Policy Scenarios to Secure Sustainability against Population Explosion: Strategy to Cope with Water Variability in Monsoon-Asia Region Managing Flood and Water-Related Risks: A Challenge for the Future. 2004. Available online: https://www.researchgate.net/publication/237407294 (accessed on 1 December 2019).
22. Wang, P.; Zhu, Y.; Yu, P. Assessment of Urban Flood Vulnerability Using the Integrated Framework and Process Analysis: A Case from Nanjing, China. *Int. J. Environ. Res. Public Health* **2022**, *19*, 16595. [CrossRef]
23. Balica, S.F.; Douben, N.; Wright, N.G. Flood vulnerability indices at varying spatial scales. *Water Sci. Technol.* **2009**, *60*, 2571–2580. [CrossRef]
24. Park, S.; Kang, B. Differentiating Scheme for the Storm Warning Criteria Considering the Regional Disaster Prevention Capacity. *J. Korean Soc. Hazard Mitig.* **2014**, *14*, 67–76. [CrossRef]
25. Kim, Y.; Choi, D.; Chang, D.; Yoo, H.; Jin, G. An improvement on the Criteria of Special Weather Report for Heavy Rain Considering the Possibility of Rainfall Damage and the Recent Meteorological Characteristics. *J. Atmos.* **2011**, *21*, 481–495.
26. Dave, H.; ME, J. Characteristics of intense rainfall over Gujarat State (India) based on percentile criteria. *Hydrol. Sci. J.* **2017**, *62*, 2035–2048. [CrossRef]
27. Choi, Y.; Yi, J. Research on flood risk forecast method using weather ensemble prediction system in urban region. *J. Korea Water Resour. Assoc.* **2019**, *52*, 753–761.
28. Noymanee, J.; Nikitin, N.O.; Kalyuzhnaya, A.V. Urban Pluvial Flood Forecasting using Open Data with Machine Learning Techniques in Pattani Basin. *Procedia Comput. Sci.* **2017**, *119*, 288–297. [CrossRef]
29. Chen, J.; Li, Y.; Zhang, C.; Tian, Y.; Guo, Z. Urban Flooding Prediction Method Based on the Combination of LSTM Neural Network and Numerical Model. *Int. J. Environ. Res. Public Health* **2023**, *20*, 1043. [CrossRef]
30. Henonin, J.; Russo, B.; Mark, O.; Gourbesville, P. Real-time urban flood forecasting and modelling—A state of the art. *J. Hydroinform.* **2013**, *15*, 717–736. [CrossRef]
31. Shin, S.; Park, C. Analyzing Relationships between Land Use Characteristics and Flood Damage Areas: The Case of Seoul. *Korea Spat. Plan. Rev.* **2014**, *81*, 3–20. [CrossRef]
32. Schueler, T.R.; Holland, H.K. The Importance of Imperviousness. *Watershed Prot. Tech.* **2014**, *1*, 100–111.
33. Sheng, J.; Wilson, J.P. Watershed urbanization and changing flood behavior across the Los Angeles metropolitan region. *Nat. Hazards* **2008**, *48*, 41–57. [CrossRef]
34. Yoo, C.-S.; Kim, D.-H.; Park, S.-H.; Kim, B.-S.; Park, C.-Y. Intervention Analysis of Urbanization Effect on Rainfall Data at the Seoul Rain Gauge Station. *J. Korea Water Resour. Assoc.* **2007**, *40*, 629–641. [CrossRef]
35. Choi, Y.; Lee, E.; Ji, J.; Ahn, J.; Kim, T.; Yi, J. Development and Evaluation of the Hydropower Reservoir Rule Curve for a Sustainable Water Supply. *Sustainability* **2020**, *12*, 9641. [CrossRef]
36. Jeon, H.-S.; Choo, Y.-M. A Study on The Operation of Drainage Pump Station Considering the Water Level of Urban River to Reduce Flooding. *J. Korea Acad. Coop. Soc.* **2022**, *23*, 14–21. [CrossRef]
37. Intergovernmental Panel on Climate Change (IPCC). *Climate Change 2001: Impacts, Adaptation, and Vulnerability*; Intergovernmental Panel on Climate Change: London, UK, 2001.
38. Dodevska, Z.; Radovanović, S.; Petrović, A.; Delibašić, B. When Fairness Meets Consistency in AHP Pairwise Comparisons. *Mathematics* **2023**, *11*, 604. [CrossRef]
39. Kuo, T. A modified TOPSIS with a different ranking index. *Eur. J. Oper. Res.* **2017**, *260*, 152–160. [CrossRef]
40. Meng, Q.S. *Information Theory*; Xi'an Jiaotong University Press: Xi'an, China, 1989.
41. Qiu, W.H. *Management Decision and Applied Entropy*; China Machine Press: Beijing, China, 2002.
42. Bao, Q.; Yuxin, Z.; Yuxiao, W.; Feng, Y. Can Entropy Weight Method Correctly Reflect the Distinction of Water Quality Indices? *Water Resour. Manag.* **2020**, *34*, 3667–3674. [CrossRef]
43. Shannon, C.E. A Mathematical Theory of Communication. *Bell Syst. Tech. J.* **1948**, *27*, 623–656. [CrossRef]

44. Ha, J.; Park, H.; Chung, G. Snow Vulnerability Analysis in Jeolla-do, South Korea using Entropy Theory. *J. Korean Soc. Hazard Mitig.* **2019**, *19*, 263–271. [CrossRef]
45. Dongbeg, S. An analysis VaR for Moving Average. *Korea Int. Account. Rev.* **2005**, *12*, 121–132.
46. Cho, J.H.; Kim, H.Y. A Study on Forecasting Model based Weighted Moving Average for Cable TV Advertising Market. *J. Inf. Syst.* **2016**, *25*, 153–171. [CrossRef]
47. Danielsson, P.-E. Euclidean distance mapping. *Comput. Graph. Image Process.* **1980**, *14*, 227–248. [CrossRef]
48. Han, J.; Cho, H.J. A Study on Cluster Analysis of Mixed Data with Continuous and Categorical Variables. *Korean Data Anal. Soc.* **2018**, *20*, 1769–1780. [CrossRef]
49. Choi, C.; Kim, K. A Study on the Development of Rainfall Risk Information Considering Local Characteristics. *J. Korean Soc. Hazard Mitig.* **2020**, *20*, 237–245. [CrossRef]
50. Pilling, C. New developments at the Flood Forecasting Centre: Operations and flood risk guidance. *WIT Trans. Built Environ.* **2016**, *165*, 237–248. [CrossRef]
51. Met Office. *Hazard Manager User Guide*; Met Office: London, UK, 2022.
52. Molteni, F.; Buizza, R.; Palmer, T.N.; Petroliagis, T. The ECMWF Ensemble Prediction System: Methodology and validation. *Q. J. R. Meteorol. Soc.* **1996**, *122*, 73–119. [CrossRef]
53. Hamill, T.M.; Hagedorn, R.; Whitaker, J.S. Probabilistic Forecast Calibration Using ECMWF and GFS Ensemble Reforecasts. Part II: Precipitation. *Mon. Weather. Rev.* **2008**, *136*, 2620–2632. [CrossRef]
54. Jung, T.; Balsamo, G.; Bechtold, P.; Beljaars, A.C.M.; Köhler, M.; Miller, M.J.; Morcrette, J.-J.; Orr, A.; Rodwell, M.J.; Tompkins, A.M. The ECMWF model climate: Recent progress through improved physical parametrizations. *Q. J. R. Meteorol. Soc.* **2010**, *136*, 1145–1160. [CrossRef]
55. Cheung, K.K.W. A review of ensemble forecasting techniques with a focus on tropical cyclone forecasting. *Meteorol. Appl.* **2001**, *8*, 315–332. [CrossRef]
56. Lee, S.-H.; Seong, Y.-J.; Kim, G.-T.; Jeong, Y.-H. Appraisal of spatial characteristics and applicability of the predicted ensemble rainfall data. *J. Korea Water Resour. Assoc.* **2020**, *53*, 1025–1037.
57. Wilks, D.S. *Statistical Methods in the Atmospheric Sciences*; Elsevier: Amsterdam, The Netherlands, 1995. [CrossRef]